1-1-2013

Point of common coupling (PCC) voltage control of a grid-connected solar photovoltaic (PV) system

Brian K. Perera
University Of Wollongong, bkp389@uowmail.edu.au

Philip Ciufo
University of Wollongong, ciufo@uow.edu.au

Sarath Perera
University of Wollongong, sarath@uow.edu.au

Point of common coupling (PCC) voltage control of a grid-connected solar photovoltaic (PV) system

Abstract

In future low voltage grids, with multiple inverter interfaced sources connected, voltage regulation may become a necessary task. The potential exists for inverter interfaced sources to be deployed to regulate the voltage at the point of common coupling (PCC) of each inverter interfaced sources. The PCC voltage regulation is attainable with inverter interfaced sources by dynamically controlling the amount of reactive power injected to the power distribution grid by individual systems. In the current research, a closed-loop controller is proposed to regulate the PCC voltage of a solar photovoltaic (PV) system that is connected to a single-phase power distribution feeder (with R to X ratio greater than 1). The plant model of the PCC voltage controller of the PV system is derived considering both reactance and resistance of the network to which the PV system is connected. Three different compensators are evaluated to identify a suitable compensator for the closed-loop PCC voltage controller to regulate the PCC voltage at a given reference voltage. Simulation studies and experimental verification confirm that the theoretical approach taken to derive the control plant model of the PCC voltage controller is accurate and the procedure that is followed to design the controller is robust. The control design procedures illustrated in the current research leads to a PCC voltage control system with acceptable dynamic and steady state performance. 2013 IEEE.

Keywords

control, solar, system, point, common, coupling, grid, pv, connected, pcc, voltage, photovoltaic

Disciplines

Engineering | Science and Technology Studies

Publication Details

B. K. Perera, P. Ciufo & S. Perera, "Point of common coupling (PCC) voltage control of a grid-connected solar photovoltaic (PV) system," in 39th Annual Conference of the IEEE Inustrial Electronics Society (IECON 2013), 2013, pp. 7475-7480.

Point of Common Coupling (PCC) Voltage Control of a Grid-Connected Solar Photovoltaic (PV) System

Brian K. Perera*, *Student Member, IEEE*, Phil Ciufo, *Senior Member, IEEE* and
Sarath Perera, *Senior Member, IEEE*
Australian Power Quality and Reliability Centre,
School of Electrical, Computer and Telecommunications Engineering,
University of Wollongong, Australia.
bkp389@uowmail.edu.au*

***Abstract*—In future low voltage grids, with multiple inverter interfaced sources connected, voltage regulation may become a necessary task. The potential exists for inverter interfaced sources to be deployed to regulate the voltage at the point of common coupling (PCC) of each inverter interfaced sources. The PCC voltage regulation is attainable with inverter interfaced sources by dynamically controlling the amount of reactive power injected to the power distribution grid by individual systems. In the current research, a closed-loop controller is proposed to regulate the PCC voltage of a solar photovoltaic (PV) system that is connected to a single-phase power distribution feeder (with R to X ratio greater than 1). The plant model of the PCC voltage controller of the PV system is derived considering both reactance and resistance of the network to which the PV system is connected. Three different compensators are evaluated to identify a suitable compensator for the closed-loop PCC voltage controller to regulate the PCC voltage at a given reference voltage. Simulation studies and experimental verification confirm that the theoretical approach taken to derive the control plant model of the PCC voltage controller is accurate and the procedure that is followed to design the controller is robust. The control design procedures illustrated in the current research leads to a PCC voltage control system with acceptable dynamic and steady state performance.**

***Index Terms*—Voltage control, photovoltaic systems, modelling, voltage source converter.**

I. Introduction

Large numbers of small scale solar photovoltaic (PV) systems (0-10 kW) are being connected to the distribution level of the power grid due to fundamental changes in policies of governments and electricity utilities towards sustainable and environmentally friendly electrical power generation technologies. PV systems are integrated to the power grid via power electronic converters. With the increased number of grid-connected PV systems, ancillary services that can be obtained from PV systems by controlling power electronic converters are becoming a topic of discussion among researchers. The network voltage control by individual PV systems is such an ancillary service that is being discussed in the literature [1]–[4] and that is further explored in the current research.

This work is supported by the Australian Research Council (ARC) and Essential Energy Linkage Grant LP100100618.

PV systems are mostly integrated to the power grid via voltage source converters (VSC) [5], [6]. A VSC is capable of operating in all four quadrants. Theoretically, the voltage at the point of common coupling (PCC) of a grid-connected VSC can be dynamically regulated by controlling the reactive power injected/absorbed by the VSC to/from the power grid. Therefore the capability of a PV system that is integrated to the grid via a VSC to regulate the network voltage would enable the PV system to be utilised as a dynamic voltage regulator in the network at all times.

The sensitivity of the PCC voltage of a grid-connected PV system to active and reactive power is a function of the network impedance that is seen by the PV system at the PCC [7]. The R/X ratio of a low voltage distribution grid is generally greater than 1. Therefore the PCC voltage of a PV system that is connected to the distribution grid is sensitive to both active and reactive power injected to the grid by the PV system. As a result, if a PCC voltage controller is designed for a PV system connected to the distribution grid, both network reactance and resistance should be taken into consideration. However in the published literature, less attention has been given for developing a PCC voltage controller for a PV system connected to the power distribution grid while providing detailed design guidelines.

In order to regulate the PCC voltage of a PV system at a given reference voltage by controlling the amount of reactive power injected to the grid by the PV system, a closed-loop controller is needed. Further, to select a suitable compensator for the controller and tuning the controller to obtain the desired response, the dynamics of the control plant of the PCC voltage controller should also be known. Therefore, in the current research, a control plant model of the PCC voltage controller of a PV system, that is integrated to a single-phase power distribution grid via a VSC, is first derived. Both reactance and resistance of the power distribution grid are taken into consideration in deriving the plant model. A closed-loop controller is proposed to regulate the PCC voltage at a given reference voltage. Further, a suitable compensator for the closed-loop PCC voltage controller is also identified among three different compensators that are evaluated. The results of simulation studies performed with integrating the developed controller to

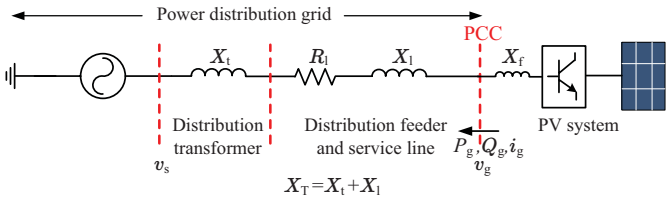

Fig. 1. Simplified model of the distribution grid.

the simulation model of the grid-connected single-phase PV system modelled in [8] are presented to verify the accuracy of the developed PCC voltage controller. Further, simulation results are verified with laboratory experiments.

In the current research, while designing the PCC voltage controller for a PV system, only a single-phase PV system that is connected to the power distribution grid is considered. The effects of the dynamic behaviour of loads and other inverter interfaced sources connected to the power distribution grid on the performance of the designed PCC voltage controller are not considered. Analysing the performance of the designed PCC voltage controller in the presence of dynamics in the power distribution grid is out of the scope of the current research. Such analysis will be performed while extending the research work presented in this paper.

This paper is organised in the following format. In Section II, the model of the distribution feeder that is considered in designing the PCC voltage controller is described. The requirement for decoupling and the technique used for decoupling the PCC voltage controller and the DC-link voltage controller of the PV system are discussed in Section III. In Section IV the derivation of the control plant model of the PV system is presented. Finally, in Section V, the proposed closed-loop PCC voltage controller is explained while identifying a suitable compensator for the controller. In Section VI the performance of the designed PCC voltage controller is verified with experimental results and conclusions are given in Section VII.

II. Simplified Model of a Distribution Feeder

A PV system that is interfaced to the power distribution grid via a VSC is considered in developing the PCC voltage controller. The effects of the dynamic behavior of loads and other inverter interfaced sources connected to the power distribution grid are not considered while designing the controller. The model of the distribution feeder considered while designing the PCC voltage controller is shown in Fig. 1. The low voltage grid is modelled with an equivalent Thévenin voltage source and a series impedance X_t. The instantaneous voltage of the Thévenin voltage source is v_s. If the impedances of high and medium voltage lines and transformers are assumed negligible, the equivalent impedance of the grid, X_t is the reactance of the distribution transformer. The distribution feeder and the service lines are modelled as a series resistance (R_l) and reactive (X_l) impedance.

The PV system is connected to the power distribution grid via an LCL filter which is a part of the PV system. The LCL filter is represented as a reactance X_f in Fig. 1. The PV system is considered to inject a real power of P_g and a reactive power of Q_g which corresponds to a current i_g into the PCC. The instantaneous voltage at the PCC is v_g.

The reference impedance for low voltage public supply systems given in [9] for electrical apparatus testing purposes is used to model the power distribution grid. Therefore in the simplified model of the single-phase power distribution feeder shown in Fig. 1, $R_T + jX_T = (0.4 + j0.25)\ \Omega$ where $R_T = R_l$ and $X_T = (X_l + X_t)$. Hence the ratio, R_T/X_T is approximately 1.6 for the considered network to which the PV system is connected.

III. Decoupling of Controllers

An expression for the PCC voltage rise, ΔV where $\Delta V = V_g - V_s$ (V_g and V_s are the rms values of v_g and v_s in Fig. 1 respectively), when the PV system is injecting P_g and Q_g to the grid, can be derived as given in (1) [7] using Fig. 1.

$$\Delta V = \frac{P_g R_T + Q_g X_T}{V_g} \tag{1}$$

The active power injected to the grid by the PV system is controlled by the DC-link voltage controller [8]. As proposed in the current research, the PCC voltage controller is designed to regulate the PCC voltage by controlling the reactive power injected to (or in fact absorbed from) the grid by the PV system. As per (1), the PCC voltage, V_g is sensitive to both active and reactive power injected to the grid by the PV system since the ratio R/X of the considered grid is greater than 1. As a result, the DC-link voltage controller and the PCC voltage controller are dynamically coupled. Thus, there should be a decoupling mechanism for the DC-link voltage controller and the PCC voltage controller of the PV system to avoid any dynamic interactions between the controllers.

The PCC voltage controller and the DC-link voltage controller can be dynamically decoupled if the grid impedance is measured or estimated [10]. In order to decouple the controllers in this manner, an algorithm to measure or estimate the grid impedance should be built into the controller. Another way of decoupling the controllers is to make the response time of one controller relatively larger than the response time of the other controller [11]. With the difference in the response times of the two controllers, the dynamics can be decoupled. A first-order lag element can be applied to change the response time of controllers [12]. Alternatively if the controllers are closed-loop control systems, the desired response time can be obtained by tuning compensators if applicable. Since there is no algorithm to measure or estimate the grid impedance built into the controller of the PV system that is modelled in [8] the latter decoupling technique that makes the response of one controller relatively slower than the response time of the other controller is used for decoupling purposes.

In order to decouple two dynamic systems, 2–10 times difference in the response times of the dynamic systems is adequate [11]. Therefore in the grid-connected PV system shown in Fig. 1, the PCC voltage controller is made ten times slower than the DC-link voltage controller in order to decouple the dynamics of the two controllers.

IV. Control plant model of the PCC voltage controller

In grid-connected PV systems a phase-locked-loop (PLL) is used to find the phase angle and the magnitude of the PCC voltage. The response time of the PLL is relatively short compared to that of the DC-link voltage controller [8]. Since the PCC voltage controller is made even slower than the DC-link voltage controller to decouple the dynamics between two controllers, the dynamics of the PLL are ignored in deriving the control plant model. Therefore the angle deviations of the PCC voltage due to reactive power injection in order to regulate the PCC voltage can be disregarded while considering only the PCC voltage magnitude deviations due to reactive power injection to the grid by the PV system.

From Fig. 1,

$$v_{\mathrm{g}} - v_{\mathrm{s}} = L_{\mathrm{T}} \frac{di_{\mathrm{g}}}{dt} + R_{\mathrm{T}} i_{\mathrm{g}}. \tag{2}$$

In (2), $L_{\mathrm{T}} = X_{\mathrm{T}}/\omega$ where ω is the nominal power frequency. A small perturbation around an operating point of the PV system where the PCC voltage controller is in the transient phase of regulating the PCC voltage at a given reference voltage is considered. With an increase in the reactive current absorbed by the PV system, (2) is modified as in (3) where Δi_{g} is the change in reactive current and Δv_{g} is the deviation of v_{g} resulting from Δi_{g}.

$$v_{\mathrm{g}} - \Delta v_{\mathrm{g}} - v_{\mathrm{s}} = L_{\mathrm{T}} \frac{d}{dt}(i_{\mathrm{g}} + \Delta i_{\mathrm{g}}) + R_{\mathrm{T}}(i_{\mathrm{g}} + \Delta i_{\mathrm{g}}) \tag{3}$$

The large and small signal components of (3) can be separated. Hence,

$$-\Delta v_{\mathrm{g}} = L_{\mathrm{T}} \frac{d}{dt}(\Delta i_{\mathrm{g}}) + R_{\mathrm{T}}(\Delta i_{\mathrm{g}}). \tag{4}$$

If the variables of (4) are expressed in the exponential form, assuming v_{g} and $-\Delta v_{\mathrm{g}}$ are in phase since the PLL of the controller of the PV system acts faster than the PCC voltage controller, then,

$$-\Delta V_{\mathrm{gm}} e^{j\omega t} = L_{\mathrm{T}} \frac{d}{dt}(\Delta I_{\mathrm{gq}} e^{j(\omega t - \frac{\pi}{2})}) + R_{\mathrm{T}}(\Delta I_{\mathrm{gq}} e^{j(\omega t - \frac{\pi}{2})}), \tag{5}$$

where ΔV_{gm} is the magnitude of Δv_{g}, ωt is the phase angle of v_{g} and ΔI_{gq} is the magnitude of Δi_{g}. Simplifying (5) further leads to (6).

$$-\Delta V_{\mathrm{gm}} = -jL_{\mathrm{T}} \frac{d}{dt}(\Delta I_{\mathrm{gq}}) + \omega L_{\mathrm{T}} \Delta I_{\mathrm{gq}} - jR_{\mathrm{T}} \Delta I_{\mathrm{gq}} \tag{6}$$

Separating real and imaginary components of (6) and considering only the real components leads to (7).

$$\Delta V_{\mathrm{gm}} = -\omega L_{\mathrm{T}} \Delta I_{\mathrm{gq}}, \tag{7}$$

The Laplace transformation of (7) leads to the plant model of the PCC voltage controller that is given in (8).

$$G_{V_{\mathrm{g}}}(s) = \frac{\Delta V_{\mathrm{gm}}(s)}{\Delta I_{\mathrm{gq}}(s)} = -\omega L_{\mathrm{T}} \tag{8}$$

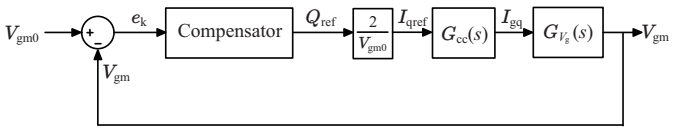

Fig. 2. Control block diagram of the PCC voltage controller.

V. Control of the PCC voltage with a dynamic reactive power controller

The design of the PCC voltage controller is described in this section. Three different types of compensators are taken into consideration for designing the controller. The control plant model of the PCC voltage controller is used for designing and tuning compensators where applicable.

The proposed closed-loop PCC voltage controller is shown in Fig. 2, where the error signal e_{k} is the difference in the magnitude of the reference PCC voltage V_{gm0} and the magnitude of the measured PCC voltage V_{gm}, $G_{\mathrm{cc}}(s)$ is the closed-loop current controller of the PV system and finally $G_{V_{\mathrm{g}}}(s)$ is the control plant model of the PCC voltage controller. Q_{ref}, I_{qref} and I_{gq} are the reactive power reference, the magnitude of the reactive current reference and the magnitude of the reactive current injected to the grid respectively.

The response time for the DC-link voltage controller of the PV system is longer than that of the current controller [8]. Further, the PCC voltage controller should be made slower than the DC-link voltage controller to decouple the two controllers. Hence, the dynamics of the current controller can be disregarded assuming $G_{\mathrm{cc}}(s) = 1$ when designing the PCC voltage controller. In Fig. 2, only the peak reactive current I_{gq} is shown as the output of $G_{\mathrm{cc}}(s)$ since the PCC voltage is controlled by regulating I_{gq} or the reactive power Q_{g} injected to the grid. But in the actual current controller of the PV system that is developed in the stationary reference frame with a proportional resonant (PR) regulator, both active and reactive current are controlled by one controller [8].

A. PCC Voltage Controller - With a Proportional Gain

The PCC voltage controller is first evaluated with only a proportional gain as the compensator in the controller. The closed-loop transfer function of the PCC voltage controller with a proportional gain is purely a gain since the plant model of the PCC voltage controller that is given in (8) is only a gain. Therefore, the PCC voltage controller cannot be made slower than the DC-link voltage controller (the transfer function of the closed-loop DC-link voltage controller of the PV system is given by (9) [8]) using only a proportional gain in the control loop.

$$G_{V_{\mathrm{dc\_cl}}}(s) = \frac{1}{0.02s + 1} \tag{9}$$

Furthermore, as there is no integrator in the plant model for the PCC voltage derived in (8), zero steady-state error cannot be achieved with only a proportional gain. Therefore, the PCC voltage controller with a proportional gain as the compensator, is not suitable for regulating the PCC voltage.

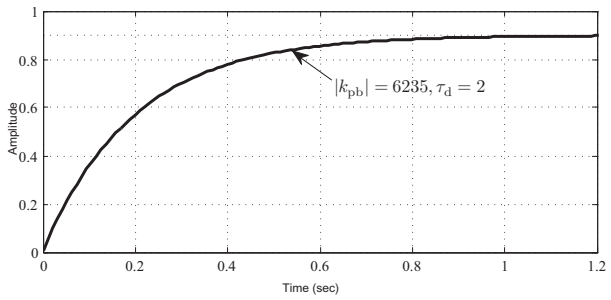

Fig. 3. Step response of the closed-loop PCC voltage controller with a proportional gain and a first-order lag element.

B. PCC Voltage Controller - With a Proportional Gain and a First-Order Lag Element

In this section, the PCC voltage controller is evaluated using a combination of a proportional gain, $k_{\rm pb}$ and a first-order lag element, $G_{\rm d}(s)$ as the compensator in the control loop of the PCC voltage controller. $G_{\rm d}(s)$ is given in (10) where $\tau_{\rm d}$ is its time constant.

$$G_{\rm d}(s) = \frac{1}{\tau_{\rm d} s + 1} \tag{10}$$

The closed-loop transfer function of the PCC voltage controller with $k_{\rm pb}$ and $G_{\rm d}(s)$ in the control loop, is given in (11).

$$G_{V_{\rm g}\_{\rm clpd}}(s) = \frac{2k_{\rm pb}G_{\rm d}(s)G_{V_{\rm g}}(s)}{V_{\rm gm0} + 2k_{\rm pb}G_{\rm d}(s)G_{V_{\rm g}}(s)} \tag{11}$$

Equation (11) can be simplified as,

$$G_{V_{\rm g}\_{\rm clpd}}(s) = \left(\frac{K_{\rm pb}}{K_{\rm pb}+1}\right)\frac{1}{\left(\frac{\tau_{\rm d}}{K_{\rm pb}+1}\right)s + 1}, \tag{12}$$

where,

$$K_{\rm pb} = \frac{2k_{\rm pb}G_{V_{\rm g}}(s)}{V_{\rm gm0}}.$$

The DC gain of (12) cannot be made equal to unity. Therefore, a steady-state error exists in the PCC voltage controller with a proportional gain and a first-order lag element. If the steady-state error is designed to be 10%,

$$\frac{K_{\rm pb}}{K_{\rm pb}+1} = 0.9,\ K_{\rm pb} = 9 \text{ and } k_{\rm pb} = -6235.$$

Equation (12) is a first-order lag element with a DC gain. Hence the desired response time of the PCC voltage controller can be achieved by placing the pole of (12) appropriately. As per (9), the time constant of the DC-link voltage controller of the PV system, $G_{V_{\rm dc\_cl}}(s)$ is 0.02 s. Therefore, in order to make the response time of the PCC voltage controller ten times larger than the DC-link voltage controller,

$$\frac{\tau_{\rm d}}{K_{\rm pb}+1} = 0.2 \text{ and } \tau_{\rm d} = 2.$$

The step response of (12) for 10% steady-state error is shown in Fig. 3.

The performance of the PCC voltage controller, with a proportional gain and a first-order lag element has been evaluated with the simulation model of the PV system modelled in [8].

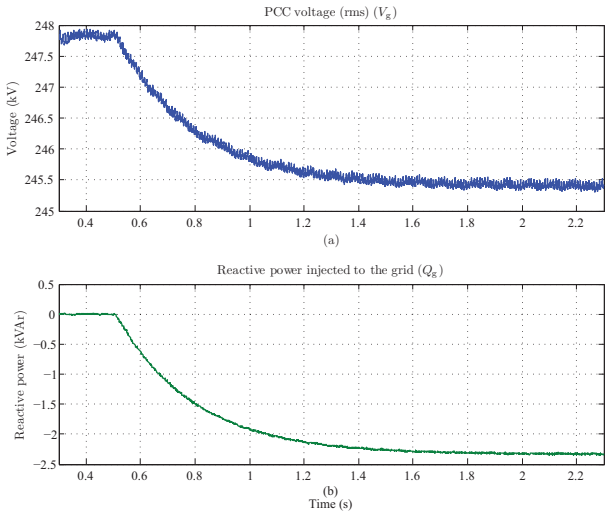

Fig. 4. PCC voltage variation-PCC voltage controller with a proportional gain and a first-order lag element.

The PCC voltage reference was set as $V_{\rm gm0} = 245\sqrt{2}$ V in the controller. The calculated values for $k_{\rm pb}$ and $\tau_{\rm d}$ were used in the simulation study and the results are shown in Fig. 4. In the simulation, initially the PCC voltage controller was not enabled and the rms value of the PCC voltage was approximately 248 V. At time $t = 0.5$ s, the PCC voltage controller was enabled. As shown in Fig. 4, the designed controller has been able to regulate the PCC voltage approximately at 245.5 V.

In the simulation, the steady-state of the PCC voltage has been reached approximately within 1 s after the PCC voltage controller was enabled. Since the time constant of (12) is 0.2 s, the steady-state PCC voltage has been reached within five time constants. This observation confirms the accuracy of the plant model of the PCC voltage controller that was derived.

C. PCC Voltage Controller - With a Proportional Gain and an Integrator

A zero steady-state error can be achieved by the PCC voltage controller only if the open-loop transfer function of the controller contains at least a pole that is closer to the origin. In order to place a pole that is closer to the origin in the open-loop transfer function of the PCC voltage controller, an integrator with a scalar can be used as the compensator shown in Fig. 2. The closed-loop transfer function of the PCC voltage controller with a scaled integrator as the compensator can be derived as,

$$G_{V_{\rm g}\_{\rm cli}}(s) = \frac{2k_{\rm pc}G_{V_{\rm g}}(s)}{V_{\rm gm0}s + 2k_{\rm pc}G_{V_{\rm g}}(s)}, \tag{13}$$

where $k_{\rm pc}$ is the scalar of the integrator. Equation (13) can be simplified as,

$$G_{V_{\rm g}\_{\rm cli}}(s) = \frac{1}{K_{\rm pc}s + 1}, \tag{14}$$

where,

$$K_{\rm pc} = \frac{V_{\rm gm0}}{2k_{\rm pc}G_{V_{\rm g}}(s)}.$$

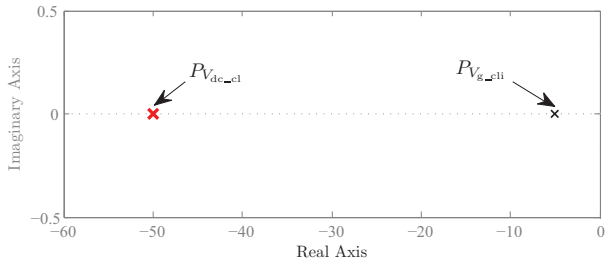

Fig. 5. Pole-zero plot of the PCC voltage controller with a scaled integrator and the DC-link voltage controller.

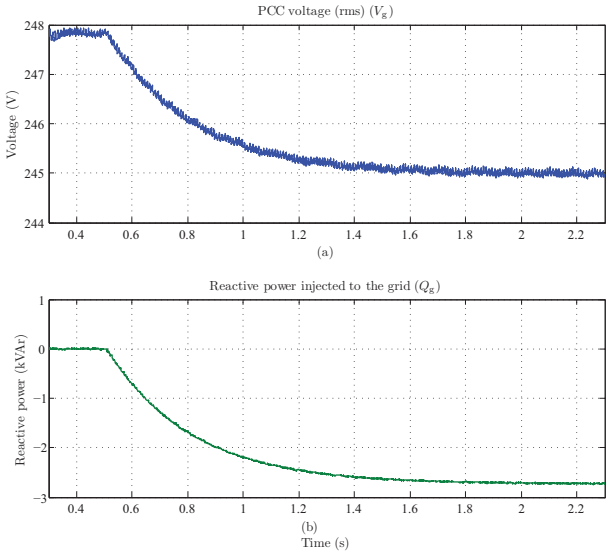

Fig. 6. PCC voltage variation-PCC voltage controller designed with a scaled integrator as the compensator.

The pole of $G_{V_{g\_cli}}(s)$ is selected as one tenth of the pole of $G_{V_{dc\_cl}}$ in (9). Therefore,

$$K_{pc} = 0.2 \text{ and } k_{pc} = -3465.$$

The pole-zero plot of (14) (the pole is labelled as $P_{V_{g\_cli}}$) with the reference grid impedance and when $k_{pc} = -3465$ is shown in Fig. 5. The location of the pole of the DC-link voltage controller (labelled as $P_{V_{dc\_cl}}$) as given in (9) is also shown in Fig. 5.

The performance of the PCC voltage controller is evaluated with the simulation model of the PV system. The PCC voltage reference of the controller was set as $V_{gm0} = 245\sqrt{2}$ V. Simulation results are shown in Fig. 6. Initially, the PCC voltage controller was not enabled and at $t = 0.5$ s the controller was enabled. As shown in Fig. 6(a), the controller is able to regulate the PCC voltage at the reference voltage. The steady-state value has been reached within 1 s. Since the PCC voltage controller with a scaled integrator is capable of driving the steady-state error to zero while effectively decoupling the PCC voltage controller and the DC-link voltage controller, a scaled integrator is a suitable compensator for the PCC voltage controller.

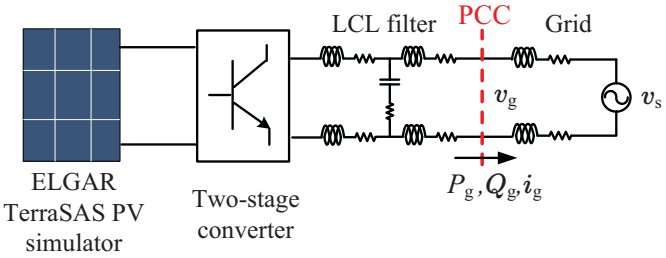

Fig. 7. A simplified block diagram of the experimental setup.

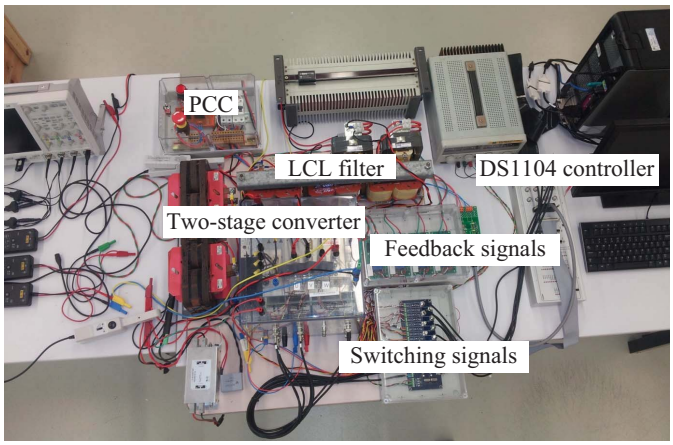

Fig. 8. A picture of a part of the experimental setup.

VI. Experimental Results

The experimental verification of the PCC voltage controller that is implemented with a scaled integrator (and described in Section V-C) are provided in this section. The practical results were obtained with an experimental setup of a grid-connected single-phase, two-stage photovoltaic system established in the laboratory. A simplified block diagram of the established experimental setup is given in Fig. 7 and a picture of a part of the experimental setup is shown in Fig. 8. In [8] the simulation model of the implemented experimental setup can be found.

In the experimental setup, the power distribution grid was simulated with an electronic power source that is connected in series with an impedance. California Instruments MX30 AC and DC power source in combination with OMNI $3-75$ impedance bank was used to simulate the power distribution grid. The impedance of the simulated grid was $(0.25 + j0.25)\ \Omega$.

The PCC voltage controller that is illustrated in Fig. 2 was built into the control system of the experimental PV system. A scaled integrator was used as the compensator. Since the plant model of the PCC voltage controller consists only the reactance of the grid impedance as shown in (8) and the reactance of the grid impedance as used in the experimental setup and simulation studies performed in Section V-C are similar, a gain of -3465 (as calculated in Section V-C) in combination with an integrator was used as the compensator of the PCC voltage controller. Though the resistance of the grid impedance used in the experimental setup and simulation studies were different, that difference does not have any significant effect on the controller performance.

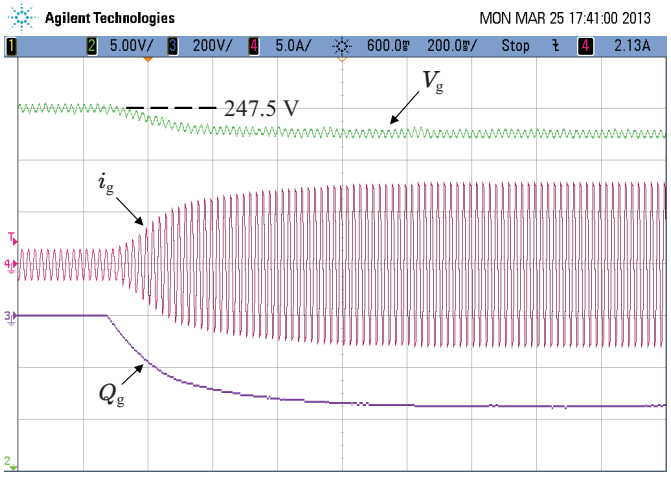

Fig. 9. Performance of the PCC voltage controller designed with a scaled integrator: Ch2: PCC rms voltage (V_g) [5 V/div], Ch3: reactive power injected to the grid (Q_g) [1 kVAr/div], Ch4: current injected to the grid (i_g) [5 A/div].

The experimental results are shown in Fig. 9. The rms voltage at the PCC of the PV system, V_g, and the amount of reactive power injected to the grid by the PV system, Q_g were obtained through the controller of the PV system. These quantities were displayed on an oscilloscope via digital to analog (D/A) conversion channels. The small ripple that can be seen in the waveform of V_g is a consequence of a small DC shift added to the sampled PCC voltage, v_g during analog to digital (A/D) conversion in the controller.

In the experimental results shown in Fig. 9, initially the PCC voltage controller was inactive and the PV system was injecting a small amount of active power to the grid. In the PCC voltage controller the reference voltage was set as $245\sqrt{2}$ V. Before activating the controller V_g was approximately 247.5 V. As shown in Fig. 9, after activating the controller, steady-state operation has been reached within about 1 s and V_g decreased to approximately 245 V. The reactive power absorbed from the grid increased to 1.75 kVAr from zero and the peak-peak value of the current injected to the grid, i_g increased to 15 A from an initial value of 2.5 A.

The experimental results shown in Fig. 9 are in good agreement with the simulation results presented in Section V-C. This demonstrate the accuracy of the plant model of the PCC voltage controller and the validity of the design procedure presented in the paper.

VII. Conclusions

The proposed closed-loop controller for a PV system that is connected to the distribution grid is capable of regulating the point of common coupling (PCC) voltage of the PV system at a given reference voltage by controlling the amount of reactive power injected to the grid by the PV system. In order to accurately regulate the PCC voltage at a given reference, a suitable compensator should be included in the controller. Among three different compensators that are evaluated in the study, the scaled integrator is found as the most suitable compensator for regulating the PCC voltage of the PV system at a given reference voltage leading to zero steady-state error. The derived plant model of the PCC voltage controller is accurate since the dynamics of the designed PCC voltage controller are predictable.

The proposed dynamic PCC voltage control scheme can be used to examine potential control interactions that can take place in multiple PV installations in a low voltage distribution feeder.

References

[1] T. Stetz, F. Marten, and M. Braun, "Improved low voltage grid-integration of photovoltaic systems in Germany," *IEEE Trans. Sustain. Energy*, vol. 4, no. 2, pp. 534–542, Apr. 2013.

[2] R. K. Varma, E. M. Siavashi, B. Das, and V. Sharma, "Novel application of a PV solar plant as STATCOM (PV-STATCOM) during night and day in a distribution utility network: Part 2," in *Proc. IEEE PES Transmission and Distribution Conf. and Exposition (T&D)*, May 2012, pp. 1–8.

[3] E. Demirok *et al.*, "Local reactive power control methods for overvoltage prevention of distributed solar inverters in low-voltage grids," *IEEE Trans. Photovoltaics*, vol. 1, no. 2, pp. 174–182, Oct. 2011.

[4] T. Stetz, W. Yan, and M. Braun, "Voltage control in distribution systems with high level PV-penetration -improving absorption capacity for PV systems by reactive power supply," in *Proc. 25th European Photovoltaic Solar Energy Conf. and Exhibition*, Sep. 2010, pp. 5000–5006.

[5] T. Kerekes, M. Liserre, R. Teodorescu, C. Klumpner, and M. Sumner, "Evaluation of three-phase transformerless photovoltaic inverter topologies," *IEEE Trans. Power Electron.*, vol. 24, no. 9, pp. 2202–2211, Sep. 2009.

[6] S. B. Kjaer, J. K. Pedersen, and F. Blaabjerg, "A review of single-phase grid-connected inverters for photovoltaic modules," *IEEE Trans. Ind. Appl.*, vol. 41, no. 5, pp. 1292–1306, Sep./Oct. 2005.

[7] R. Tonkoski, L. A. C. Lopes, and T. H. M. El-Fouly, "Coordinated active power curtailment of grid connected PV inverters for overvoltage prevention," *IEEE Trans. Sustain. Energy*, vol. 2, no. 2, pp. 139–147, Apr. 2011.

[8] B. K. Perera, S. R. Pulikanti, P. Ciufo, and S. Perera, "Simulation model of a grid-connected single-phase photovoltaic system in PSCAD/EMTDC," in *Proc. IEEE Int. Conf. on Power System Technology (POWERCON)*, Oct. 2012, pp. 1–6.

[9] "Electromagnetic Compatibility (EMC) - Consideration of reference impedance and public supply network impedances for use in determining disturbances characteristics of electrical equipment having a rated current $\leq$ 75 A per phase," IEC, Tech. Rep. TR 60725, Jun. 2012.

[10] K. De Brabandere *et al.*, "A voltage and frequency droop control method for parallel inverters," *IEEE Trans. Power Electron.*, vol. 22, no. 4, pp. 1107–1115, Jul. 2007.

[11] A. Yazdani and R. Iravani, *Voltage-Sourced Converters in Power Systems*. Wiley/IEEE, 2010.

[12] E. Demirok, D. Sera, R. Teodorescu, P. Rodriguez, and U. Borup, "Evaluation of the voltage support strategies for the low voltage grid connected pv generators," in *Proc. IEEE Energy Conversion Congress and Exposition (ECCE)*, Sep. 2010, pp. 710–717.